Graphical Abstract

Two novel entangled POM-based coordination polymers have been successfully hydrothermal synthesized. Compound **1** represents an unprecedented 2D+2D→3D polypseudorotaxane motif, while compound **2** exhibits a self-catenated framework with multi-form helical chains. Photocatalysis experiments reveal that both compound **1** and **2** can prohibit the photodegradation of Methylene Blue (MB).
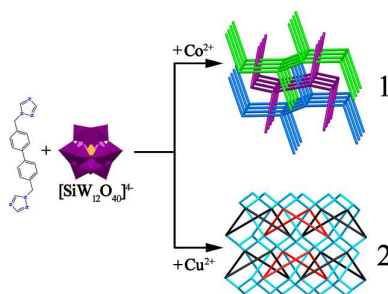
Two unprecedented entangled coordination polymers based on

α-{SiW$_{12}$O$_{40}$}$^{4-}$

Yu-Hui Luo[a], Xiao-Yang Yu[a, b] and Hong Zhang[a]

[a] Institute of Polyoxometalate Chemistry, Department of Chemistry, Northeast Normal University,

Changchun, Jilin 130024, P. R. China

[b] College of Chemical and Pharmaceutical Engineering, Jilin Institute of Chemical Technology,

Jilin City, Jilin, 132022, P. R. China

* E-mail: zhangh@nenu.edu.cn (H. Zhang)

Abstract: Two novel entangled POM-based coordination polymers (CPs), namely, [Co$_2$(L)$_5$(H$_2$O)$_2$(SiW$_{12}$O$_{40}$)] (**1**), [Cu$_2$(L)$_3$(H$_2$O)$_2$(SiW$_{12}$O$_{40}$)]·H$_2$O (**2**) (L = 4,4'-bis((1H-1,2,4-triazol-1-yl)methyl)biphenyl), have been hydrothermally synthesized. Compound **1** represents an unprecedented 2D+2D→3D polypseudorotaxane motif. The fascinating self-catenated framework of compound **2** contains three types of helical chains. In addition, photocatalysis properties of compounds **1** and **2** have also been investigated.

Introduction

Polyoxometalates (POMs), a class of nanosized transition-metal oxide clusters, are attracting more and more interests for their virtually unmatched range of properties.[1] It is this unique range of properties that qualifies POMs as desirable building blocks for the designed construction of functional materials with applications in, for instance, magnetism, electrochemistry and catalysis.[2] The construction of functional POM-based coordination polymers (CPs) is usually achieved by using one-pot synthetic method in the presence of organic linkers or ligand-supported metal moieties. Although scores of POM-based CPs have been reported, the rational syntheses of those with special structural features, such as entangled POM-based CPs, remain as challenges.

Entanglements, including interpenetration, interdigitation, polycatenation, polythreading, and other species, have attracted considerable attention due to their aesthetic structures and potential applications arising from the intertwining structure.[3] As defined by Ciani and his coworkers,[4] the main feature of polycatenation is that its dimensionality increase with the presence of interlocked loops. While polythreaded systems can be considered as extended periodic analogues of the molecular rotaxanes or *pseudo*-rotaxanes. Although numerous of entangled frameworks with complicated structure have been reported in recent years, only six types of POM-based polypseudorotaxanes have been reported (Scheme 1).[5] Consequently, the construction of new kinds of POM-supported polypseudorotaxanes is still a difficult task in POM chemistry. It has been noticed that CPs are more likely to produce polythreaded framework in the presence of rigid and flexible ligands.[6] In this respect, Keggin-type silicotungstic acid ($H_4SiW_{12}O_{40} \cdot xH_2O = H_4SiW_{12}$) can be considered as the rigid ligand. Firstly, the rigid atomic cluster contains as many as 36 surface oxygen atoms, which can display multiple bridging modes to coordinate to metal ions. Secondly, the surface oxygen atoms of H_4SiW_{12} can also act as hydrogen bonding acceptors to stable the final structure. On the other hand, flexible N-donor ligands with excellent coordination   ability,   such   as   1,3-di(pyridin-4-yl)propane,

1,4-di(1H-imidazol-1-yl)butane and 1,4-bis((1H-imidazol-1-yl)methyl)benzene, have also been proven to be suitable to the construction of entangled networks.[7]
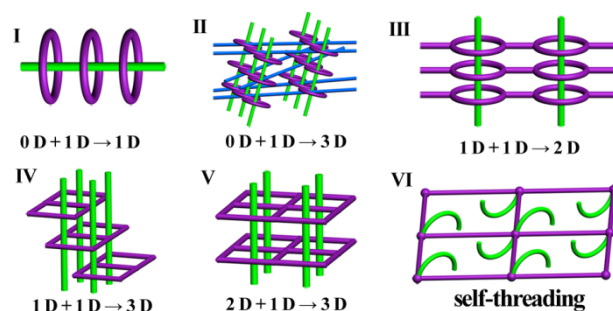
Scheme 1 Schematic representations of the reported POM-based polypseudorotaxanes.

In this work, we try to utilize the long flexible N-donor ligand, 4,4'-bis((1H-1,2,4-triazol-1-yl)methyl)biphenyl (L), and Keggin-type H_4SiW_{12} to assemble entangled CPs under hydrothermal conditions. Two novel entangled POM-based CPs, namely, $[Co_2(L)_5(H_2O)_2(SiW_{12}O_{40})]$ (**1**), $[Cu_2(L)_3(H_2O)_2(SiW_{12}O_{40})]\cdot H_2O$ (**2**), have been successfully synthesized. Structural analyses indicate that the two-dimensional (2D) layers of **1** are interdigitated giving rise to an unprecedented 2D+2D→3D polypseudorotaxane motif, while compound **2** shows three-dimensional (3D) self-catenated framework with the presence of multi-form helical chains. In addition, photocatalysis properties of **1** and **2** have also been studied.

L
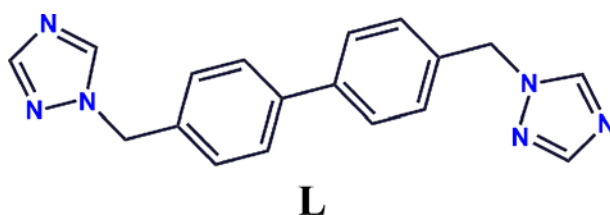
Scheme 2 Structure of the ligand used in this work.

Experimental section

Materials and general methods. All reagents and solvents were purchased from commercial sources and used without further purification. The FI-IR spectra were measured in KBr pellets in the range 4000–400 cm^{-1} on a Mattson Alpha-Centauri spectrometer. Elemental analysis (EA) for C, H and N was performed on a Perkin-Elmer 2400 Elemental Analyzer. Thermogravimetric analysis (TGA) was

performed on a Perkin-Elmer Thermal Analyzer under nitrogen atmosphere at a heating rate of 10 °C min^{-1}. The UV absorption was measured with a Cary 500 UV-Vis-NIR Spectrophotometer. Powder X-ray diffraction (PXRD) patterns were collected on a Rigaku D_{max} 2000 X-ray diffractometer with graphite monochromatized Cu-$K\alpha$ radiation (λ = 0.15418 nm) and 2θ ranging from 5 to 50 ° with an increment of 0.02 °.

Preparation of [Co$_2$(L)$_5$(H$_2$O)$_2$(SiW$_{12}$O$_{40}$)] (1). A mixture of CoCl$_2$·6H$_2$O (0.1 mmol, 24.0 mg), H$_4$SiW$_{12}$ (0.02 mmol, 60 mg), L (0.05 mmol, 15 mg) and H$_2$O (10 mL) was stirred at room temperature for about 4 hours. And the pH of the mixture was adjusted to about 3.5 by adding one drop of hydrochloric acid (1 mol/L). Then the mixture was transferred into a 23 mL Teflon-lined stainless steel autoclave reactor and heated at 160 °C for 72 hours. After cooled to room temperature at a rate of 10 °C·h^{-1}, orange block crystals suitable for X-ray structural analysis were isolated by ultrasonically cleaned, washed with water several times, dried in air, and handpicked. Yield: *ca.* 25 % (based on H$_4$SiW$_{12}$). Anal. calcd for C$_{90}$H$_{84}$Co$_2$N$_{30}$O$_{42}$SiW$_{12}$ (%): C, 23.45; H, 1.84; N, 9.12. Found: C, 23.41; H, 1.82; N, 9.09. IR (KBr, cm^{-1}): v = 3471 (m), 3112 (m), 1614 (s), 1539 (m), 1432 (m), 1387 (m), 1339 (m), 1278 (m), 1221 (s), 1168 (s), 1078 (s), 965 (s), 910 (s), 782 (s), 685 (s), 480 (m).

Preparation of [Cu$_2$(L)$_3$(H$_2$O)$_2$(SiW$_{12}$O$_{40}$)]·H$_2$O (2). The preparation of **2** is similar to that of **1** except that CuCl$_2$·2H$_2$O (0.1 mmol, 17.0 mg) was used instead of CoCl$_2$·6H$_2$O. Green block crystals were collected in a yield of 42 % (based on H$_4$SiW$_{12}$). Anal. calcd for C$_{54}$H$_{54}$Cu$_2$N$_{18}$O$_{43}$SiW$_{12}$ (%): C, 16.20; H, 1.36; N, 6.30. Found: C, 16.23; H, 1.32; N, 6.35. IR (KBr, cm^{-1}): v = 3462 (m), 3126 (m), 1618 (s), 1528 (s), 1438 (m), 1385 (m), 1336 (m), 1275 (m), 1227 (s), 1171 (s), 1075 (s), 968 (s), 911 (s), 786 (s), 678 (s), 520 (m).

Photocatalysis experiments. The experiment with a typical process, 15 mg of **1** or **2** was added in 350 mL Methylene Blue (MB) solutions (5 × 10^{-5} mol L^{-1}) and then the solutions were magnetically stirred in the dark for 30 min. The mixture was then exposed to UV irradiation under stirring continuously, and 2.0 mL of solution was taken out every 7 min for analysis.

X-ray crystallography. Crystallographic diffraction date for **1** and **2** were performed on an Oxford Diffraction Gemini R Ultra diffractometer at 293 K, using a graphite monochromated Mo-$K\alpha$ radiation (λ = 0.71073 Å). Both of the structures were refined by full-matrix least-squares techniques using the SHELXL-97 program.[8] All non-hydrogen atoms were refined with anisotropic temperature parameters and all hydrogen atoms on organic ligands were placed in geometrically idealized position as a riding mode. The water hydrogen atoms (except for O2W in **2**) cannot be located from difference Fourier maps. The disordered atoms were splited over two sites with a total occupancy of 1. And all these disordered atoms were restricted by SIMU and ISOR. Some bond lengths (N3A-N2 and N3B-N2 in **1**) were restricted by DFIX. In addition, the atoms (Si1 and O4 in **1**; C3, C8, C9, C10, C13, C18, C19, C21, C23, C24, C26, C27, N9, O1, O2, O3, O4, O7, O14, O18 and Si1 in **2**) with ADP were also restricted by ISOR. The crystallographic data for **1** and **2** are shown in Table 1.

Table 1 Crystal data and structure refinements for **1** and **2**.

Compounds	**1**	**2**
Formula	$C_{90}H_{84}Co_2N_{30}O_{42}SiW_{12}$	$C_{54}H_{54}Cu_2N_{18}O_{43}SiW_{12}$
M_r	4610.02	4004.52
Temp (K)	293(2)	293(2)
Wavelength (Å)	0.71073	0.71073
Crystal system	Monoclinic	Orthorhombic
Space group	$P2_1/c$	$Pccn$
a (Å)	16.3042(11)	12.6869(7)
b (Å)	22.6007(8)	22.7919(14)
c (Å)	17.1913(9)	28.5112(19)
α (deg)	90	90
β (deg)	115.290(7)	90
γ (deg)	90	90
V (Å^3)	5727.6(5)	8244.3(9)
Z	2	4
$F(000)$	4252	7232
R_{int}	0.0530	0.0572
GOF	1.078	1.060

R_1 $[I>2\sigma(I)]^a$	0.0682	0.0834
wR_2 (all data)^a	0.1111	0.1566

$^a R_1 = \sum ||F_0| - |Fc||/\sum |F_0|$; $wR_2 = \sum [w(F_0^2 - Fc^2)^2]/\sum [w(F_0^2)^2]^{1/2}$.

Results and discussion

Crystal structure of 1. Structural analysis indicates that **1** exhibits an unprecedented 2D+2D→3D polypseudorotaxane framework. The asymmetric unit of **1** contains one Co(II) ion, two and a half L ligands, half $\{SiW_{12}\}^{4-}$ anion and one coordination water molecule. The Si atom of the $\{SiW_{12}\}^{4-}$ anion lies on an inversion centre, with concomitant disorder of the four oxygen atoms (O1, O2, O3, O4) which are directly bonded to it. As shown in Fig. 1a, Co1 is six-coordinated in a distorted octahedral coordination geometry, defined by four nitrogen atoms from four L molecules, one oxygen atom from one $\{SiW_{12}\}^{4-}$ anion and one coordination water molecular (Co–N 2.07(2)-2.13(2) Å, Co–O 2.097(14)-2.157(13) Å). Co(II) ions are linked into a one-dimensional (1D) chain by μ_2-L ligands along the *a* axis (Fig. 1b). Then, the 1D chains are further connected by bi-supported $\{SiW_{12}\}^{4-}$ clusters to generate a 2D 4^4-**sql** layer with projecting mono-coordinated L ligands on both sides (Fig. 1d and S1a). It is easy to find that the 2D layer in **1** contains two types of windows (Fig. 1c). The first type of windows (type I) are formed by four L ligands connecting four Co ions, while the second type of windows (type II) are integrated by four Co ions, two μ_2-L ligands and two $\{SiW_{12}\}^{4-}$ anions. Layers of **1** are alternately arranged in an *ABA* fashion with windows I face to windows II of the adjacent layers (Fig. S1b and S1c). Interestingly, windows II, with suitable size, can be simultaneously threaded by two mono-coordinated lateral arms from two adjacent layers (Fig. S1e). Thus, an unusual 2D+2D→3D polypseudorotaxane network is formed (Fig. 2). As shown in Scheme S1, compared with the reported 2D+2D→3D polythreaded framework,[9] compound **1** represents a different type of 2D+2D→3D polypseudorotaxane motif. As far as we know, **1** is also the first POM-based compound with 2D+2D→3D polypseudorotaxane framework.
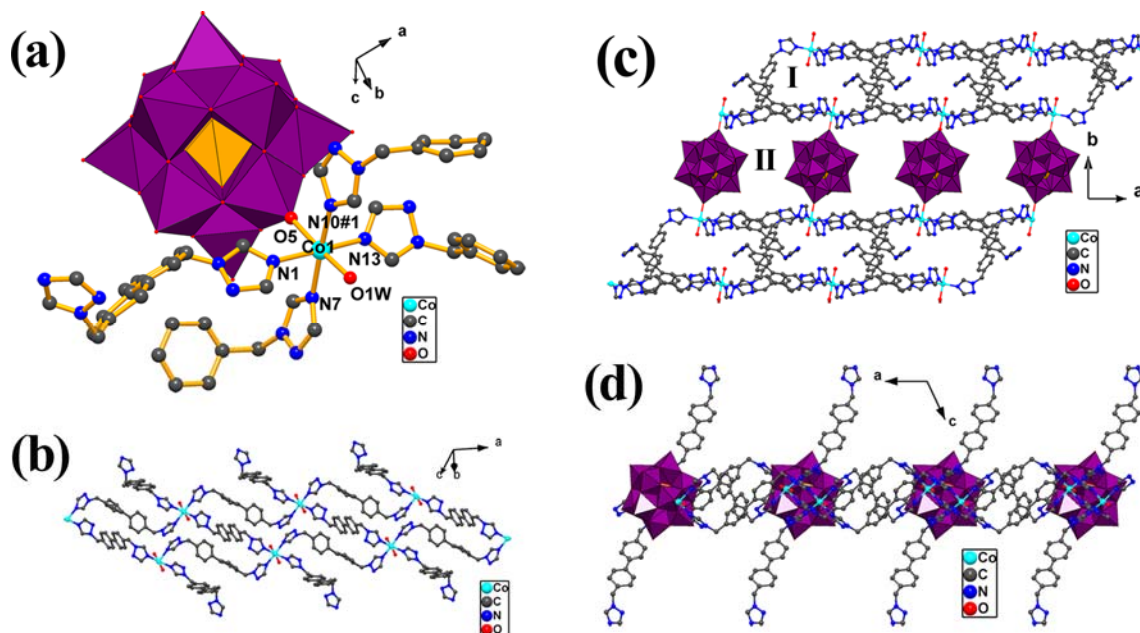
Fig. 1 (a) Coordination environment of Co1 ion in **1**. Symmetry codes: #1, 1+x, y, z. (b) View of 1D chain constructed by μ_2-L ligands connecting Co ions. (c) The 2D 4^4-**sql** layer of **1** contains two kinds of windows. (d) View of the projecting mono-coordinated L ligands on both sides of the layer. $\{SiW_{12}\}^{4-}$ anions in (a), (c) and (d) are depicted as polyhedral representative. All hydrogens are omitted for clarity.
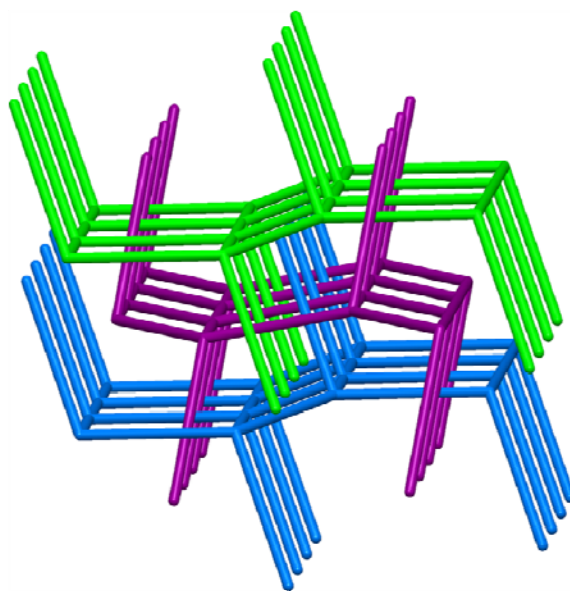
Fig. 2 Schematic illustration of the 2D+2D→3D polypseudorotaxane motif of **1**.

A further study on the structure shows that non-bonding interactions, such as hydrogen bonds, $\pi\cdots\pi$ interactions and C−H$\cdots\pi$ interactions, play important roles in the formation of the 3D supramolecular architecture of **1**. The 2D layers are connected by O1W$\cdots$N5 hydrogen bonds (O1W$\cdots$N5 2.735(6) Å) to generate a 3D

interpenetrating framework with 2-fold **pcu** topology (Fig. 3a and Fig. S2).[10] Otherwise, as shown in Fig. 3b, face-to-face $\pi\cdots\pi$ interactions (face-to-face distance of 3.71 Å and centroid-to-centroid distance of 3.89 Å) and C16−H16A$\cdots\pi$ interactions (C16$\cdots$Cg(2): 3.42(3) Å; Cg(2): C4, C5, C6, C7 ,C8, C9) between the two mono-coordinated lateral arms, which are fixed in the same windows, also help to stable the 3D supramolecular architecture. The detail parameter of these non-bonding interactions are listed in Table S1-S3.
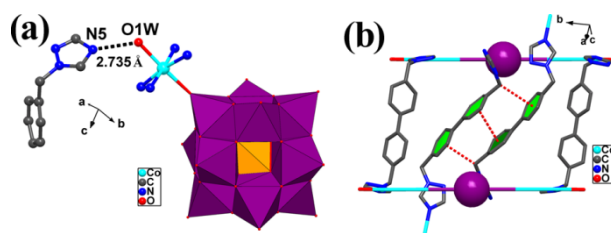
Fig. 3 (a) Representation of O1W$\cdots$N5 hydrogen-bonding interaction. The $\{SiW_{12}\}^{4-}$ anion is depicted as polyhedral representative. (b) Illustration of $\pi\cdots\pi$ and C−H$\cdots\pi$ interactions (shown in red dashed line) between the mono-coordinated L ligands. The big purple balls in (b) represent $\{SiW_{12}\}^{4-}$ anions. All hydrogens are omitted for clarity.

Crystal structure of 2. It is well known that metal ions can significantly affect the final structures due to their different size and coordination geometry.[11] Herein, when we replaced the $CoCl_2\cdot6H_2O$ with $CuCl_2\cdot2H_2O$, compound **2** was prepared with a different framework. Single-crystal X-ray diffraction analysis reveals that **2** shows a 3D self-catenated network with the presence of three types of helical chains. The asymmetric unit of **2** contains one Cu(II) ion, one and a half L ligands, half $\{SiW_{12}\}^{4-}$ anion, one coordination water molecule and half solvent water molecule. The Si atom of the $\{SiW_{12}\}^{4-}$ anion lies on a two-fold axis, with concomitant disorder of the four oxygen atoms (O1, O2, O3, O4) which are directly bonded to it. The L ligand with C22 lies on an inversion centre (at the midpoint of the biphenyl moiety). In addition, water oxygen atom O2W lies on a two-fold axis. As shown in Fig. 4a, Cu1 is six-coordinated by three nitrogen atoms from three L molecules, two oxygen atoms from two different $\{SiW_{12}\}^{4-}$ clusters and one oxygen atom from one coordination water molecular, showing a distorted octahedral coordination geometry (Cu–N 1.95(2)-2.299(19) Å, Cu–O 2.01(2)-2.652(2) Å). Cu ions are connected by μ_2-L

ligands to generate a 1D inter-connected double-*meso*-helical chain along the *b* axis (Fig. 4b, 4d and 4e). Afterward, the chains are catenated into a 2D layered structure (Fig. 4c). The 2D layers are further linked into a 3D structure by tetra-supported $\{SiW_{12}\}^{4-}$ clusters (Fig. S2b). Interestingly, another two types of helical chains, running along the *a* axis, can also been found in the 3D structure of **2**. The second type helical chains are double-standard *meso*-helical chains integrated by Cu ions, $\{SiW_{12}\}^{4-}$ anions and L ligands (Fig. 4f and 4g). The third type helical chains contain racemic left- and right-handed single-helical chains, which is constructed from Cu ions and $\{SiW_{12}\}^{4-}$ anions (Fig. 4h and 4i). From the topological view, each Cu ion connected two $\{SiW_{12}\}^{4-}$ clusters and three other Cu ions can be considered as a 5-connected node. Each $\{SiW_{12}\}^{4-}$ anions connected four Cu ions can be considered as a 4-connected node. Thus the 3D framework of **2** can be reduced to a binodal (4,5)-connected net with $(4 \cdot 6 \cdot 8^4)(4^4 \cdot 6^4 \cdot 8^2)_2$ topology (Fig. S2c-e).[10] More fascinatingly, the framework of **2** displays a self-penetrating phenomenon, that is, the shortest four-membered rings catenate to adjacent ones giving rise to a self-catenated motif (Fig. 5). As far as we know, compound **2** is the first self-catenated POM-based CPs with multi-form helical chains.
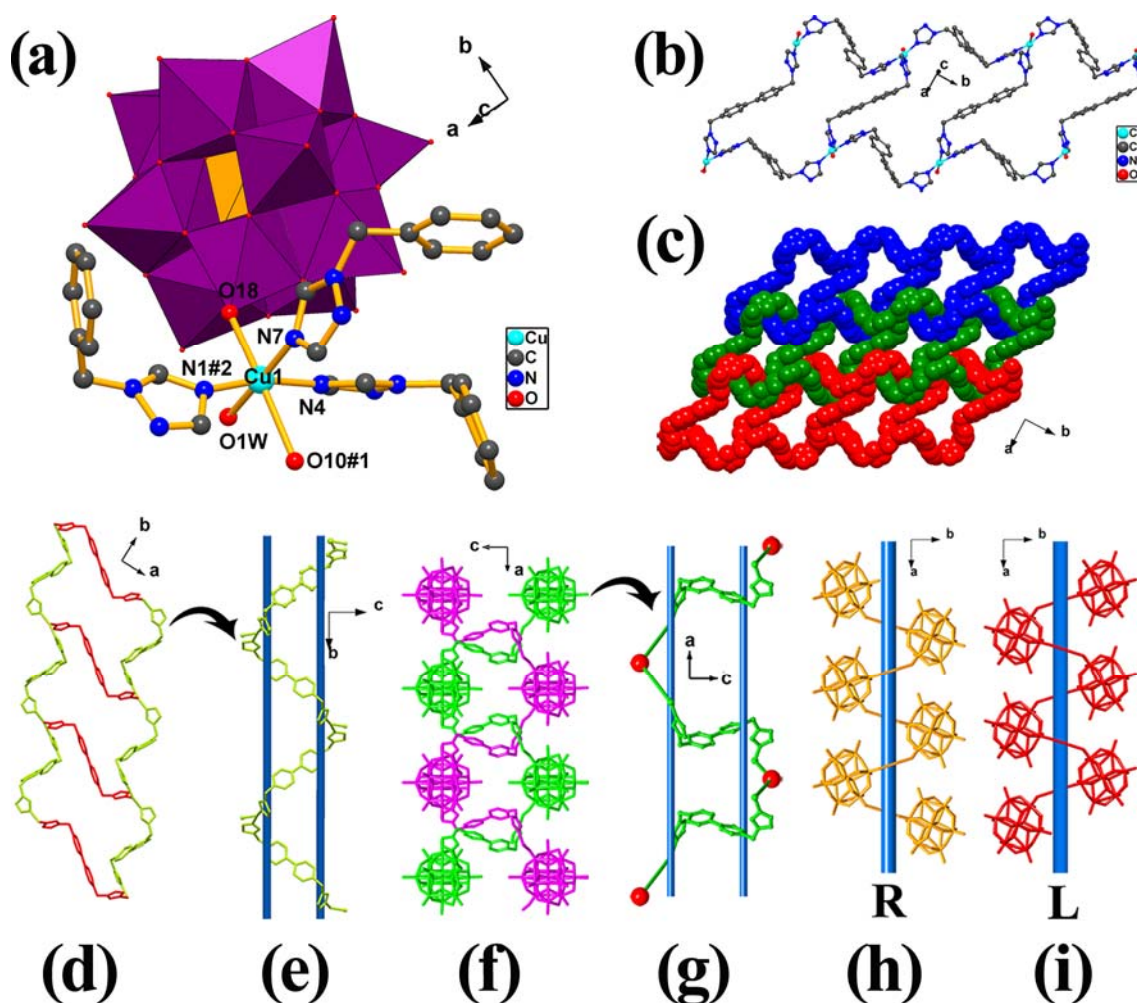
Fig. 4 (a) Coordination environment of Cu1 ion in **2**. The $\{SiW_{12}\}^{4-}$ anion is depicted as polyhedral representative. Symmetry codes: #1, $1/2+x$, $1-y$, $1/2-z$; #2, $1/2+x$, $1/2+y$, $-z$. (b) View of 1D ladder-shape chain constructed by μ_2-L ligands connecting Cu ions. (c) Space-filling representation of the 2D layered structure knitted by 1D chain. (d) and (e) View of the 1D inter-connected double-*meso*-helical chain. (f) and (g) View of the double-standard *meso*-helical chains. The big red balls in (g) represent $\{SiW_{12}\}^{4-}$ anions. (h) and (i) View of the racemic left- and right-handed single-helical chains. All hydrogens are omitted for clarity.
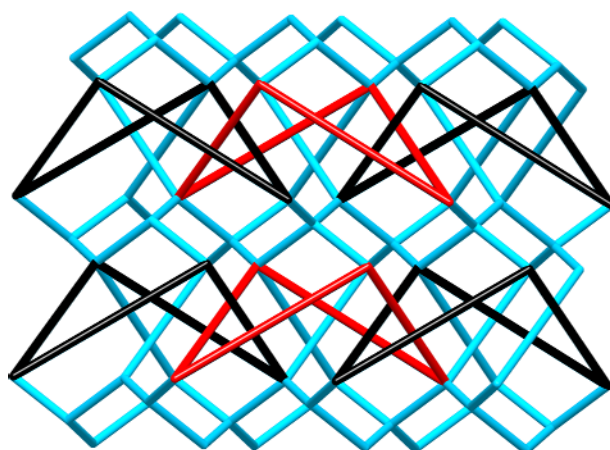
Fig. 5 Topological view of **2**. The shortest interlocked 4-membered rings are highlighted in black and red.

Photocatalysis experiments. The photocatalysis properties of **1** and **2** have been investigated with photodegradation reactions of MB under UV light irradiation. As shown in Fig. S6a and S6b, the absorption peak of MB decreases as the irradiation time increases, which indicates that MB gradually decomposition. The peak positions of the tested PXRD patterns of **1** and **2** after photocatalysis experiments are respectively in good agreement with those of the as-synthesized samples, indicating their high structural stability during the UV irradiation (Fig. S7). The degradation of MB in the presence of **1**, **2** and no catalyst upon irradiation for 49 min is 70.3 %, 62.2 % and 80.6 %, respectively. This result reveals that the degradation rate of the MB in the presence of **1** or **2** is slower than that in the absence of photocatalysts (Fig. 6). In other words, both **1** and **2** can prohibit the photodegradation of MB. In order to explain these phenomena, the decomposition process of MB in the presence of $CoCl_2 \cdot 6H_2O$ (2.0 mg/350ml), $CuCl_2 \cdot 2H_2O$ (1.8 mg/350 mL) or H_4SiW_{12} (10 mg/350 mL) has also been investigated. It's easy to find that the degradation rate of the MB reduced with the presence of $CuCl_2 \cdot 2H_2O$ (Fig. 6). This indicated that the presence of $CuCl_2 \cdot 2H_2O$ in the solution can effectively prohibit the photoinduced degradation of MB. Otherwise, when H_4SiW_{12} was added as catalyst, the absorption spectra of the solution changed and only a little decreases of the absorption peak can be found as the irradiation time increases (Fig. S6f). This suggests the association of MB molecules and $\{SiW_{12}\}^{4-}$ anions. The association may be arisen from the hydrogen-bonding interactions between MB molecules and $\{SiW_{12}\}^{4-}$ clusters.[12] Otherwise, MB performs as bulk organic cations can also associate with $\{SiW_{12}\}^{4-}$ anions through electrostatic attraction. These interactions may enhance the chemical stability of MB molecules in the solution. Furthermore, according to the reported work, H_4SiW_{12} can be reduced by radical.[13] In this work, the radical $MB^{\cdot +}$ may be oxidized by H_4SiW_{12}.[14] Then, the number of the radical was decreased and the degradation rate of MB was reduced. Thus, the inhibition of the photodegradation of MB in the presence of **1** or **2** may be attributed to: i) the oxidation of radical in the presence of $\{SiW_{12}\}^{4-}$; ii) the

association of MB molecules and photocatalysts; iii) the presence of Cu(II) in the structure of **2**.[13, 15]
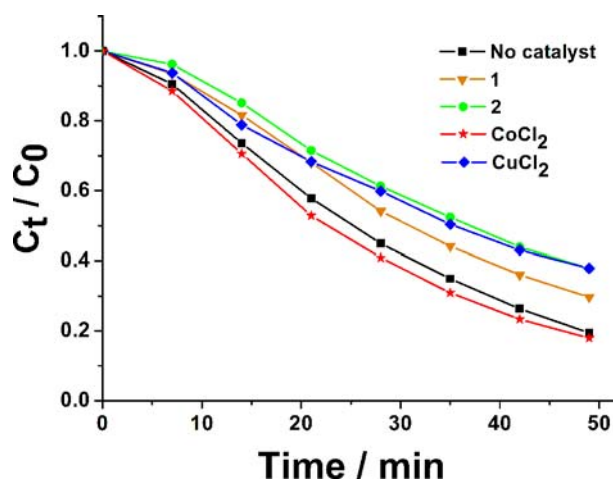
Fig. 6 Concentrations of MB under UV light irradiation.

Conclusion

Two unusual entangled POM-based coordination polymers (CPs) have been successfully synthesized via the hydrothermal method. Structural analyses reveal that compound **1** represents a new type of 2D+2D→3D polypseudorotaxane motif. In comparison, compound **2** exhibits a 3D self-catenated framework with the presence of three types of helical chains. The successful preparation of **1** and **2** provides valuable clues on the systematically assembly of entangled frameworks based on POM.

Electronic supplementary information (ESI) available

Crystallographic files (CIF), structure diagrams, PXRD patterns, TGA curves, tables of hydrogen bonds and selected bond lengths and angles. CCDC reference number: 979329 (**1**), 979330 (**2**). For ESI and crystallographic data in CIF or other electronic format see DOI: xxxx

Acknowledgements

References

1 (a) M. T. Pope and A. Müller, *Angew. Chem., Int. Ed.*, 1991, **30**, 34; (b) L. Cronin and A. Muller, *Chem. Soc. Rev.*, 2012, **41**, 7333; (c) U. Kortz and T. Liu, *Eur. J. Inorg. Chem.*, 2013, 1559; (d) U. Kortz, A. Müller, J. V. Slageren, J. Schnack, N. S. Dalal, M. Dressel, *Coordin. Chem. Rev.*, 2009, **253**, 2315; (e) N. V. Izarova, M. T. Pope, U. Kortz, *Angew. Chem., Int. Ed.*, 2012, **51**, 9492; (f) D. L. Long, E. Burkholder, L. Cronin, *Chem. Soc. Rev.*, 2007, **36**, 105.

2 (a) D. L. Long, R. Tsunashima, L. Cronin, *Angew. Chem., Int. Ed.*, 2010, **49**, 1736; (b) S. T. Zheng, J. Zhang, G. Y. Yang, *Angew. Chem., Int. Ed.*, 2008, **47**, 3909; (c) A. M.Khenkin, I. Efremenko, J. M. L. Martin, R. Neumann, *J. Am. Chem. Soc.*, 2013, **135**, 19304; (d) F. J. Ma, S. X. Liu, C. Y. Sun, D. D. Liang, G. J. Ren, F. Wei, Y. G. Chen, Z. M. Su, *J. Am. Chem. Soc.*, 2011, **133**, 4178; (e) P. Huang, C. Qin, Z. M. Su, Y. Xing, X. L. Wang, K. Z. Shao, Y. Q. Lan, E. B. Wang, *J. Am. Chem. Soc.*, 2012, **134**, 14004; (f) G. Gao, F. Li, L. Xu, X. Liu, Y. Yang, *J. Am. Chem. Soc.*, 2008, **130**, 10838; (g) S. G. Mitchell, C. Streb, H. N. Miras, T. Boyd, D. L. Long, L. Cronin, *Nature Chem.*, 2010, **2**, 308.

3 (a) S. R. Batten, B. F. Hoskins, R. Robson, *Chem. Eur. J.*, 2000, **6**, 156; (b) J. Yang, J. F. Ma, S. R. Batten, *Chem. Commun.*, 2012, **48**, 7899; (c) T. K. Maji, R. Matsuda, S. Kitagawa, *Nature Mater.*, 2007, **6**, 142; (d) X. H. Bu, M. L. Tong, H. C. Chang, S. Kitagawa, S. R. Batten, *Angew. Chem., Int. Ed.*, 2004, **43**, 192; (e) Y. Y. Liu, H. Y. Liu, J. F. Ma, Y. Yang, J. Yang, *CrystEngComm*, 2013, **15**, 1897; (f) M. D. Zhang, C. M. Di, L. Qin, Q. X. Yang, Y. Z. Li, Z. J. Guo, H. G. Zheng, *CrystEngComm*, 2013, **15**, 227; (g) G. P. Yang, L. Hou, L. F. Ma, Y. Y. Wang, *CrystEngComm*, 2013, **15**, 2561; (h) O. M. Yaghi, *Nature Mater.*, 2007, **6**, 92; (i) R. Kitaura, K. Seki, G. Akiyama, S. Kitagawa, *Angew. Chem., Int. Ed.*, 2003, **42**, 428.

4 L. Carlucci, G. Ciani, D. M. Proserpio, *Coordin. Chem. Rev.*, 2003, **246**, 247.

5 (a) B. X. Dong, Q. Xu, *Cryst. Growth Des.*, 2009, **9**, 2776; (b) H. J. Pang, H. Y. Ma, J. Peng, C. J. Zhang, P. P. Zhang, Z. M. Su, *CrystEngComm*, 2011, **13**, 7079; (c) P. P. Zhang, A. X. Tian, J. Peng, H. J. Pang, J. Q. Sha, Y. Chen, M. Zhu, Y. H. Wang, *Inorg. Chem. Commun.*, 2009, **12**, 902; (d) H. Wu, J. Yang, Y. Y. Liu, J. F. Ma, *Cryst. Growth Des.*, 2012, **12**, 2272; (e) J. H. Liao, J. S. Juang, Y. C. Lai, *Cryst. Growth Des.*, 2005, **6**, 354; (f) Q. G. Zhai, X. Y. Wu, S. M. Chen, Z. G. Zhao, C. Z. Lu, *Inorg. Chem.*, 2007, **46**, 5046; (g) J. L. Zambrana, E. X. Ferloni, J. C. Colis, H. D. Gafney, *Inorg. Chem.*, 2007, **47**, 2; (h) W. Q. Kan, J. F. Ma, Y. Y. Liu, H. Wu, J. Yang, *CrystEngComm*, 2011, **13**, 7037.

6 (a) J. Yang, J. F. Ma, S. R. Batten, Z. M. Su, *Chem. Commun.*, 2008, 2233; (b) B. F. Hoskins, R. Robson, D. A. Slizys, *Angew. Chem., Int. Ed.*, 1997, **36**, 2336.

7 (a) K. L. Huang, X. Liu, J. K. Li, Y. W. Ding, X. Chen, M. X. Zhang, X. B. Xu, X. J. Song, *Cryst. Growth Des.*, 2010, **10**, 1508; (b) D. Sun, M. Z. Xu, S. S. Liu, S. Yuan, H. F. Lu, S. Y. Feng, D. F. Sun, *Dalton Trans.*, 2013, **42**, 12324; (c) Y. Q. Lan, S. L. Li, J. S. Qin, D. Y. Du, X. L. Wang, Z. M. Su, Q. Fu, *Inorg. Chem.*, 2008, **47**, 10600.

8 (a) G. M. Sheldrick, *SHELXS-97:Programs for X-ray Crystal Structure Solution.* University of Göttingen, Göttingen, Germany, 1997; (b) G. M. Sheldrick, *SHELXL-97:Programs for X-ray Crystal Structure Refinement.* University of Göttingen, Göttingen, Germany, 1997.

9 (a) Y. Yang, P. Du, J. F. Ma, W. Q. Kan, B. Liu, J. Yang, *Cryst. Growth Des.*, 2011, **11**, 5540; (b) B. Xu, J. Lu, R. Cao, *Cryst. Growth Des.*, 2009, **9**, 3003; (c) Y. H. Luo, F. X. Yue, X. Y. Yu, L. L. Gu, H. Zhang, X. Chen, *CrystEngComm*, 2013, **15**, 8116; (d) Y. L. Gai, F. L. Jiang, L. Chen, Y. Bu, M. Y. Wu, K. Zhou, J. Pan, M. C. Hong, *Dalton Trans.*, 2013, **42**, 9954; (e) W. Q. Kan, J. F. Ma, Y. Y. Liu, J. Yang, *CrystEngComm*, 2012, **14**, 2316; (f) M. Du, X. G. Wang, Z. H. Zhang, L. F. Tang, X. J. Zhao, *CrystEngComm*, 2006, **8**, 788; (g) G. L. Wen, Y. Y. Wang, Y. N. Zhang, G. P. Yang, A. Y. Fu, Q. Z. Shi, *CrystEngComm*, 2009, **11**, 1519; (h) L. Y. Qiao, J. Zhang, Z. J. Li, Y. Y. Qin, P. X. Yin, J. K. Cheng, Y. G. Yao, *J. Mol. Struct.*, 2011, **994**, 1; (i) C. Qin, X. L. Wang, L. Carlucci, M. L. Tong, E. B. Wang, C. W. Hu, L. Xu, *Chem. Commun.*, 2004, 1876.

10 V. A. Blatov, *Struct. Chem.*, 2012, **23**, 955.

11 (a) Y. Li, W. Q. Zou, M. F. Wu, J. D. Lin, F. K. Zheng, Z. F. Liu, S. H. Wang, G. C. Guo, J. S. Huang, *CrystEngComm*, 2011, **13**, 3868; (b) H. L. Wang, L. F. Zhang, Z. H. Ni, W. F. Zhong, L. J. Tian, J. Z. Jiang, *Cryst. Growth Des.*, 2010, **10**, 4231; (c) A. Q. Wu, Y. Li, F. K. Zheng, G. C. Guo, J. S. Huang, *Cryst. Growth Des.*, 2006, **6**, 444; (d) D. P. Zhang, H. L. Wang, L. J. Tian, H. Z. Kou, J. Z. Jiang, Z. H. Ni, *Cryst. Growth Des.*, 2009, **9**, 3989.

12 J. Niu, S. Zhang, H. Chen, J. Zhao, P. Ma, J. Wang, *Cryst. Growth Des.*, 2011, **11**, 3769.

13 L. Q. Ma, Y. L. Yang, Y. Z. Wang, R. Q. Fan, Y. Ding, *Hua Xue Tong Bao*, 1998, **61**, 56.

14 Y. Yang, Q. Y. Wu, Y. H. Guo, C. W. Hu, E. B. Wang, *J. Mol. Catal. A-Chem.*, 2005, **225**, 203.

15 D. L. Sedlak, J. Hoigné, M. M. David, R. N. Colvile, E. Seyffer, K. Acker, W. Wieprecht, J. A. Lind, S. Fuzzi, *Atmos. Environ.*, 1997, **31**, 2515.